Available online at www.sciencedirect.com
ScienceDirect
ELSEVIER
European Journal of Medical Genetics 51 (2008) 44–53
EUROPEAN JOURNAL OF MEDICAL GENETICS
http://www.elsevier.com/locate/ejmg

Original article

Impact of geometry and viewing angle on classification accuracy of 2D based analysis of dysmorphic faces

Tobias Vollmar [a], Baerbel Maus [a], Rolf P. Wurtz [b], Gabriele Gillessen-Kaesbach [c], Bernhard Horsthemke [a], Dagmar Wieczorek [a], Stefan Boehringer [a,*]

[a] *Institut für Humangenetik, Universität Duisburg-Essen, Hufelandstrasse 55, 45122 Essen, Germany*
[b] *Institut für Neuroinformatik, Ruhr-Universität Bochum, Germany*
[c] *Institut für Humangenetik, Universität zu Luebeck, Germany*

Received 4 June 2007; accepted 6 October 2007
Available online 12 October 2007

Abstract

Digital image analysis of faces has been demonstrated to be effective in a small number of syndromes. In this paper we investigate several aspects that help bringing these methods closer to clinical application. First, we investigate the impact of increasing the number of syndromes from 10 to 14 as compared to an earlier study. Second, we include a side-view pose into the analysis and third, we scrutinize the effect of geometry information. Picture analysis uses a Gabor wavelet transform, standardization of landmark coordinates and subsequent statistical analysis. We can demonstrate that classification accuracy drops from 76% for 10 syndromes to 70% for 14 syndromes for frontal images. Including side-views achieves an accuracy of 76% again. Geometry performs excellently with 85% for combined poses. Combination of wavelets and geometry for both poses increases accuracy to 93%. In conclusion, a larger number of syndromes can be handled effectively by means of image analysis.

Keywords: Automated pattern recognition; Computer-assisted diagnosis; Classification; Dysmorphism; Face

* Corresponding author. Tel.: +49 201 723 4533; fax: +49 201 723 5900.
E-mail address: correspondence@s-boehringer.org (S. Boehringer).

1769-7212/$ - see front matter © 2007 Elsevier Masson SAS. All rights reserved.
doi:10.1016/j.ejmg.2007.10.002

1. Introduction

Syndrome diagnosis based on clinical examination of patients is a challenge in everyday clinical practice [16]. Databases are an integral part of this process complementing clinical expertise [14,17]. In the past we have shown that computer-based analysis of frontal pictures of faces might be a helpful addition to this process. We introduced a method of computer-based syndrome diagnosis based on 2D pictures processed by wavelet picture analysis and subsequent statistical analysis [3,12]. By means of wavelet analysis, a sparse, yet informative, representation of a picture can be achieved [13,18,19]. To optimize face analysis, information is focused on certain landmarks in the face (*model graph*; Fig. 1). Using *model graphs*, a classification accuracy of ~75% can be achieved among 10 syndromes [3], which roughly equals the performance of an ad hoc diagnosis by clinicians in a previous study [12]. As a consequence of growing data complexity accuracy decreases as more syndromes are included (compare [3,12]). Therefore, it seems mandatory to enrich the data set with additional information. It is straightforward to include side-views of faces which harbor, both, unique clinical features like ear and chin but also contribute three-dimensional information. An additional strategy is to include geometry information, which is based on landmark coordinates. Geometry seems to be an important feature in human face recognition and processing [2,10,11] and should therefore contribute to the distinction of syndromes. For example the stability of manual landmark placement has been demonstrated [1]. Also, many distances in the skull bone structures show significant heritability [8,9,15]. Coordinates of landmarks have been successfully employed in the analysis of 3D representation of faces [6,7]. In the cited study geometry was the sole information source. From these studies, it seems essential that landmark correspondence is good, *i.e.*, the exact positioning of nodes at predefined positions like nose-tip, lips, *etc*. [2,4,5]. This implies that standardization is required and manual positioning of landmarks improves results [3]. We have therefore opted to include geometry information into our data set by using coordinates of manually placed landmarks, followed by standardization. We compare the relative impact of wavelet information of frontal and side-views with coordinate information and consider

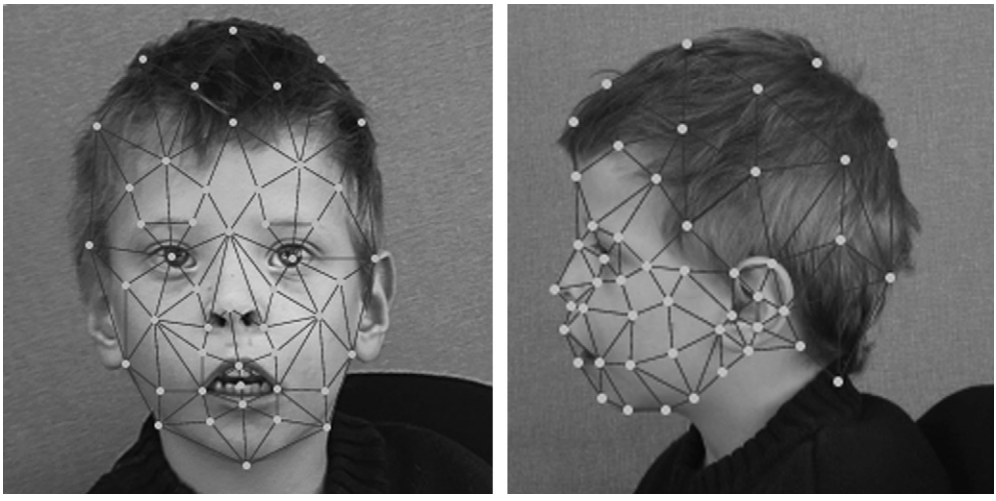

Fig. 1. Example pictures of used model graphs in front and side-view pose.

the combined data set. Finally, we use a data set of 14 syndromes which furthers our evaluation of the impact of the inclusion of more syndromes into our ongoing study.

2. Materials and methods

2.1. Probands

We acquired photographs of patients each being affected by one in 14 syndromes (Microdeletion 22q11.2, Wolf–Hirschhorn syndrome, Cri-du-chat syndrome, Cornelia de Lange syndrome, Fragile X syndrome, Mucopolysaccharidosis Type II, Mucopolysaccharidosis Type III, Noonan syndrome, Prader–Willi syndrome, Progeria, Smith–Lemli–Opitz syndrome, Sotos syndrome, Treacher Collins syndrome, Williams–Beuren syndrome). Annual meetings of parent support groups have been visited and written informed consent was given by the probands or their responsible parents. In total $n = 200$ probands were included. Probands' ages ranged from 1 to 45 years. A breakup for individual syndromes is given in Table 1. This extends our previous data set by four newly added syndromes (Wolf–Hirschhorn syndrome, Mucopolysaccharidosis Type II, Progeria, Treacher Collins syndrome; Fig. 2; for other syndromes c.f. [3]).

2.2. Picture acquisition and selection

Arrangement of the equipment and illumination of the photographic setting were standardized and reproduced as accurately as possible at the different meetings. Three lighting sources created a soft illumination and reduced shadows in the faces, which could otherwise affect later analyses. A homogeneous background was used throughout. We acquired, both, frontal and side-view pictures taken with a digital camera (Nikon Coolpix 950, Nikon Coolpix 4500) and a video sequence of a rotation of the proband around a vertical axis (Panasonic NV-MX350EG). Videos allowed for subsequent extraction of still pictures to achieve optimal pictures for both poses. Final picture selection was based on pose, sharpness and facial expression. For each individual a single picture was selected per pose.

Table 1
Characterization of the data set

Condition	Age range	Number of probands
Microdeletion 22q11.2 (22q-)	1.7–16.4	26
Wolf–Hirschhorn syndrome (4p-)	1.1–40.5	8
Cri-du-chat syndrome (5p-)	1.0–16.8	9
Cornelia de Lange syndrome	7.1–33.7	12
Fragile X syndrome	4.6–13.8	12
Mucopolysaccharidosis II	4.3–20.4	7
Mucopolysaccharidosis III	4.5–15.5	8
Noonan syndrome	0.6–37.2	15
Prader–Willi syndrome	5.0–20.9	12
Progeria	5.7–8.4	5
Smith–Lemli–Opitz syndrome	0.3–16.3	12
Sotos syndrome	1.0–20.3	15
Treacher Collins syndrome	1.6–45.3	12
Williams–Beuren syndrome	2.9–45.0	43

Fig. 2. Example pictures of the newly included syndromes in front and side-view pose (top to bottom: Wolf–Hirschhorn syndrome, Mucopolysaccharidosis Type II, Progeria, Treacher Collins syndrome).

2.3. Picture preparation and analysis

Pictures were converted to a standard format (gray scale, resolution 256×256 pixels). In a two-step analysis pictures are re-represented by *model graphs* which contain Gabor wavelet transforms of important facial features. Details of this process are given elsewhere [12,18]. In short, landmarks of the face are located in the picture based on similarity with independent example pictures and Wavelet coefficients are extracted at each landmark (48 landmarks, 40 coefficients each). Wavelet representation can be viewed as a form of image compression that allows to approximate the original image based alone on the coefficients and the position of the corresponding landmark (*i.e.*, the *model graph*) [19].

We have also created versions of the *model graphs* for which landmarks have been assigned by a human investigator (*hand-labeled model graphs*). Previous work has shown that manual intervention in landmark placement is highly accurate [1] and improves classification results [3].

2.4. Statistical analysis

In the statistical analysis we used both versions of *model graphs* (hand-labeled and automatic) of frontal and side-views. We have conducted separate and combined analyses of the two poses. Additionally, we have also analyzed the geometry and the wavelet components of *model graphs* separately and in combination.

Coordinates were standardized prior to ensuing analysis. Graph coordinates were rotated to a standard angle, centered and scaled to unit size. Because of the complexity of the data set (points and wavelets of both poses comprise $2 \times 1920 + 2 \times 96 = 4032$ coordinates per sample), dimension reduction techniques have to be employed. We used principal component analysis (PCA) to reduce dimensionality to *ca.* 100 coordinates depending on the particular data set. Recall, that PCA orders the resulting coordinates (principal components; PCs) by their relevance in explaining variance of the data set. Whenever we combined coordinates and wavelets we combined data after conducting PCA separately on the two components.

We have employed several classification techniques to assess classification accuracy. These methods were linear discriminant analysis (LDA), support vector machines (SVM) and k-th nearest neighbors (kNN). These methods differ in complexity and robustness. LDA uses a hyperplane to separate different classes. By contrast, SVM uses a maximum-margin hyperplane in conjunction with a non-linear transformation, which allows for non-linear decision boundaries. kNN uses a majority vote of the classes of the k nearest training samples to assign a class to an independent sample. Classification accuracy was defined by conducting a 10-fold cross validation procedure. Ten-fold cross validation assesses accuracy by repeatedly splitting the data set into train/test pairs, predicting unseen test samples from the training data and averaging accuracy over runs. We have averaged accuracy over 20 cross validation runs to minimize effects of random fluctuations due to hold out sample selection. We have used two model selection schemes to select PCs for classification. First, we selected the first k PCs in the k-th step (block selection). This allows to compare results with our previous study [3,12]. A more sophisticated but also more demanding algorithm in terms of computation time is forward selection. Each step adds a new PC to the set of class predictors by choosing the PC that best improves classification accuracy. Forward selection was applied to the first 90 wavelet PCs and the first 60 coordinate PCs.

3. Results

3.1. Block selection

Results for block selection in Table 2 can be directly compared to our previous study [3]. These classification results do not use coordinate information. Using LDA, classification accuracy for hand-labeled wavelets is 70.1% for 14 syndromes as compared to 76% for 10 syndromes in the previous study. Side-view pictures alone performed at 62.7% and the combination of both poses performed at 76.1%. Wavelets extracted from the automatic process performed considerably worse at 52% for frontal views. For side-views an accuracy of 42% was achieved. We note, however, that we have not updated the process locating the landmarks with more examples as compared to the previous study. SVM and *k*NN performed at 63% and 58%, respectively, and are thus worse than LDA as was the case in the previous study. For SVM 1st degree polynomials were used. *k*NN is the worst classifier in this study (front, side-view pictures or combination; data not shown) with the best accuracy achieved with $k = 6$ neighbors.

Breaking up results for individual syndromes, Fragile X syndrome (100%), progeria (99%) and Williams–Beuren syndrome (90.9%) were the syndromes with best results. Interestingly, progeria performs at only 63% for side-views alone. Syndromes with the worst accuracies were Mucopolysaccharidosis Type III in frontal pose (6.3%) and Cri-du-chat syndrome, which holds for both poses (frontal: 11%, side-view 48%). Interestingly, accuracy of Cri-du-chat syndrome performs better using only side-views.

3.2. Pairwise comparisons

For deeper insight into which distinctions are difficult to learn for the computer in the current data set we conducted pairwise classifications for all syndrome pairs. Table 3 reports

Table 2
Classification accuracies using different data sets and classification methods

Classification method	LDA				SVM	*k*NN
Picture pose	Combined	Frontal	Side-view	Frontal	Frontal	Frontal
Model graph	Manual	Manual	Manual	Automatic	Manual	Manual
Overall (%)	76.1	70.1	62.7	52.5	63.8	58.2
22q- (%)	88.1	75.4	65.0	54.2	79.6	69.8
4p- (%)	53.1	43.3	50.0	25.4	22.5	12.5
5p- (%)	32.2	11.7	48.9	18.3	16.1	0.6
Cornelia de Lange (%)	83.8	74.6	65.4	82.1	58.3	43.4
Fragile X (%)	100.0	94.6	97.5	87.8	91.7	97.6
Mucopolysaccharidosis II (%)	57.9	59.3	60.0	94.3	40.7	32.1
Mucopolysaccharidosis III (%)	6.3	35.6	6.3	0.0	8.1	17.5
Noonan (%)	77.0	79.0	51.0	51.0	58.0	78.3
Prader–Willi (%)	83.3	71.2	75.0	74.3	71.2	45.4
Progeria (%)	99.0	98.0	63.0	52.0	67.0	47.0
Smith–Lemli–Opitz (%)	59.2	59.6	20.4	25.0	55.4	44.6
Sotos (%)	80.0	71.0	77.7	63.3	61.3	37.3
Treacher Collins (%)	64.2	39.2	34.6	50.8	24.2	35.8
Williams–Beuren (%)	90.9	91.0	84.2	70.6	93.3	82.0

The third row indicates whether manually corrected or fully automatically created model graphs were used. Results for SVM use 1st degree polynomials, *k*NN $k = 6$ neighbors.

Table 3
Results of pairwise classification of frontal views using 26 PCs gained from wavelet coefficients for Microdeletion 22q (22q-), Wolf–Hirschhorn (4p-), Cri-du-chat (5p-), Cornelia de Lange (CDL), Fragile X (FraX), Mucopolysaccharidosis II (MPS2), Mucopolysaccharidosis III (MPS3), Noonan, Prader–Willi (PWS), Progeria, Smith–Lemli–Opitz Sotos (SLO), Treacher Collins (TCS) and Williams–Beuren (WBS)

	22q-	4p-	5p-	CDL	FraX	MPS2	MPS3	Noonan	PWS	Progeria	SLO	Sotos	TCS
4p- (%)	94.3	–	–	–	–	–	–	–	–	–	–	–	–
5p- (%)	85.0	91.8	–	–	–	–	–	–	–	–	–	–	–
CDL (%)	95.8	98.0	82.6	–	–	–	–	–	–	–	–	–	–
FraX (%)	99.5	98.2	90.5	76.0	–	–	–	–	–	–	–	–	–
MPS2 (%)	91.6	98.5	92.8	83.2	97.1	–	–	–	–	–	–	–	–
MPS3 (%)	84.1	90.0	63.5	93.5	93.5	54.7	–	–	–	–	–	–	–
Noonan (%)	84.8	93.4	81.3	85.2	93.7	87.7	82.0	–	–	–	–	–	–
PWS (%)	95.5	91.8	80.0	93.3	63.1	96.8	88.0	81.7	–	–	–	–	–
Progeria (%)	91.6	82.3	85.0	95.9	99.1	93.5	55.6	98.0	98.6	–	–	–	–
SLO (%)	96.2	96.5	82.6	89.8	98.7	89.4	84.4	81.5	97.7	98.9	–	–	–
Sotos (%)	86.9	96.1	65.4	72.6	96.9	85.0	74.1	59.2	93.1	90.4	81.2	–	–
TCS (%)	87.7	80.0	89.6	84.0	89.2	92.5	72.2	79.3	77.3	99.0	95.4	74.9	–
WBS (%)	95.5	98.1	95.1	97.2	98.2	98.7	97.5	97.3	94.6	100.0	97.5	91.9	95.8

accuracies for a hand-labeled data set and wavelet information from frontal pictures. Classification rates range from 54.7% (MPS II *vs*. MPS III) up to perfect discrimination (*e.g*. Progeria *vs*. Williams–Beuren syndrome). Most rates range between 80% and 100%. Mucopolysaccharidosis III is difficult to discriminate from MPS II, Progeria and Cri-du-chat with accuracies below 70%. Cri-du-chat discriminates poorly from MPS III and Sotos syndrome.

3.3. Forward selection

Forward selection was applied to geometry information, wavelets and the combination. We here report only on data sets including both poses. Table 4 summarizes the results. It is notable,

Table 4
Classification accuracies for coordinates and wavelets for combined poses (frontal and side-view)

	Geometry (%)	Wavelets (%)	Geometry + wavelets (%)
Overall	85.7	76.9	93.1
Microdeletion 22q	87.7	86.9	94.6
Wolf–Hirschhorn	80.0	57.5	97.5
Cri-du-chat	78.9	47.8	72.2
Cornelia de Lange	73.3	78.3	82.5
Fragile X	91.7	91.7	100.0
Mucopolysaccharidosis II	70.0	70.0	82.9
Mucopolysaccharidosis III	70.0	22.5	61.3
Noonan	97.3	80.0	93.3
Prader–Willi	81.7	76.7	91.7
Progeria	96.0	64.0	100.0
Smith–Lemli–Opitz	78.3	63.3	97.8
Sotos	92.0	91.3	89.3
Treacher Collins	83.3	65.8	93.7
Williams–Beuren	91.2	91.6	97.1

Classification method is LDA using forward selection and *model graphs* were *hand-labeled*.

that geometry information performs excellently and an overall accuracy of 85.7% is achieved. Wavelets perform at 76% and the combination at 93%. This indicates that non-overlapping information is contained in coordinates and wavelets, respectively. Cri-du-chat syndrome performs at 78% for geometry thereby improving over wavelet results at 47%. Also in MPS III, geometry performs well at 70% as compared to 22% with wavelets. Except for Wolf–Hirschhorn syndrome (improvement from 57% to 80%), progeria (64%, 96%) and Smith–Lemli–Opitz syndrome (63%, 78%) results were similar when comparing geometry with wavelets.

4. Discussion

One future goal of this study is to enhance databases with capabilities of image analysis. To be usable, a large number of syndromes have to be supported. This study gives some insight into the feasibility of this task. Our previous study performed at 75% for 10 syndromes. Taking into account that the probability of a correct diagnosis by random choice is 10%, this means a ratio of 7.5 comparing a-posteriori and a-priori probabilities. In the present study this ratio ranged from 8.8 (side-views, hand-labeled wavelets) to 13.0 (combined frontal side-view together with coordinates) supporting the view that significant information is carried by both side-views and geometry. Also we have shown that classification accuracy does not have to deteriorate as more syndromes are included – which is a prerequisite to moving forward to the clinical application.

It is interesting to look at the different components of the data set that were used in the classification process. Side-views seem to harbor less information than frontal views in terms of classification accuracy. However, this might not be a genuine finding but due to a particular property of our data set. For example, hair is an uncontrolled source of noise in our data set. Side-views seem to be more severely affected by this factor. Here, of course, physical examination of a patient could assess relevance much better. It should be mentioned that Prader–Willi syndrome and Sotos syndrome are more accurately classified using side-views than frontal views. Since the combination of frontal and side-views performs best, non-overlapping, complementary information should be contained in these two parts of the data set, as is expected (ears, side profile). In particular, three-dimensional information about the face can be derived from a pair of frontal and side-view pictures.

The second addition in this study was the inclusion of coordinates after standardization. Astonishingly, coordinate information results in excellent classification accuracy. This result was unexpected, since non-standardized coordinates completely failed to classify. There are two main consequences of this result. Firstly, coordinates do not harbor any texture information. In classification studies that are based on samples not drawn randomly from the population but sampled from subgroups, hidden correlations can give rise to spuriously accurate results in classification experiments. For example, subtle differences in the picture acquisition process could be systematically present in one of the groups of patients and could be the true factors for the correct classification decision. We have gone to great lengths to exclude these factors by inspecting summary statistics of pictures, plausibility checks and visualizations of the decision process [3]. The geometry result is an independent support for the correctness of the previous analyses. The second aspect is standardization. We have so far not standardized pictures by geometric transformation, since Gabor wavelets have some properties that make them robust against such transformations [18,19]. Since we want to apply our methods on pictures that are not as accurately controlled for as the ones we used in this study, we are going to rely on this robustness even more. The geometry results, however, indicate that accuracy using

wavelets can also be increased by strict standardization. Such a standardization is possible, when landmarks are positioned by hand, since this reveals the true geometry of the face. It remains to be seen how well an automated procedure can work, but we consider this to be a promising improvement.

Automatically labeled pictures have not performed well in this study.

To explain this result, two aspects are important. Firstly, in rare instances the face was not localized at all in the automatic process, thereby representing a data point with complete noise. This fact becomes more relevant as more syndromes are included, since the chance that such a point of noise lies close to one of the other syndromes increases. Therefore, mistakes like these should be avoided in the training data set that could be used in practice. Secondly, we have not optimized the localization of landmarks, since for the reasons just mentioned we have performed manual labeling, anyway. Locating landmarks can be improved by several means, including a well-chosen training set, including faces with variation in syndrome, sizes and rotation. Also algorithmic improvements are possible and currently under investigation. In conclusion, a completely automatic analysis is not feasible at the moment and landmark placement should always be checked and corrected to achieve best results.

In clinical practice, it is certainly possible to adjust landmarks for a single pair of facial pictures that is to be analyzed by hand, however, there are additional challenges that have only partially been covered thus far. One important issue is the composition of the training data set. Should only very characteristic probands be included or should also mild phenotypes be included? On the one hand, this could drive down classification accuracy in studies like this, on the other hand in practice a ranking of syndromes could be more helpful than a single decision. For example, the classifier could be indecisive between several syndromes but could be able to exclude a large number of syndromes. This could also be helpful in practice, and therefore measures other than pure classification accuracy could be useful.

This study is the first to include geometry information of 2D-pictures. It was astonishing to see, that accurate standardization can lead to excellent classification results. 3D studies that are solely based on geometry information, have shown similar results, although the data sets and analyses are not directly comparable. Combining coordinates from frontal as well as side-views seems to recover 3D-information as well, since similar results are achieved with 3D and 2D coordinates. It should be noted that 3D coordinates have not been standardized to a unit volume, which seems to be an option for a re-analysis of the 3D data set. One advantage of the 3D-approach is that coordinates are absolute, *i.e.*, sizes can be accurately reconstructed. In our data set we have to rely on surrogate information, like age, for size.

In conclusion, we believe that the current results are promising in terms of improving syndrome diagnosis in practice. Main outcomes, that are expected by us to reach clinical practice soon, are that result lists from database queries can be made more significant by excluding syndromes that are prototypically too dissimilar and giving meaningful order to lists of suggested syndromes. A high level of expertise of the clinician will still be indispensable for an accurate and reliable diagnosis.

Acknowledgments

We thank all patients who took part in the study. We thank Stella Sinigerova for helping with labeling. This study was supported by DFG grants BO 1955/2-1, WU 314/2-1 and IFORES grant 107-05860, 107-02270.

References

[1] K. Aldridge, S.A. Boyadjiev, G.T. Capone, V.B. DeLeon, J.T. Richtsmeier, Precision and error of three-dimensional phenotypic measures acquired from 3dMD photogrammetric images, Am. J. Med. Genet. A 138 (2005) 247–253.
[2] J.E. Allanson, Objective techniques for craniofacial assessment: what are the choices? Am. J. Med. Genet. 70 (1997) 1–5.
[3] S. Boehringer, T. Vollmar, C. Tasse, et al., Syndrome identification based on 2D analysis software, Eur. J. Hum. Genet. 14 (2006) 1082–1089.
[4] T.S. Douglas, Image processing for craniofacial landmark identification and measurement: a review of photogrammetry and cephalometry, Comput. Med. Imaging Graph 28 (2004) 401–409.
[5] L.G. Farkas, J.C. Posnick, T.M. Hreczko, G.E. Pron, Growth patterns of the nasolabial region: a morphometric study, Cleft Palate Craniofac. J. 29 (1992) 318–324.
[6] P. Hammond, T.J. Hutton, J.E. Allanson, et al., Discriminating power of localized three-dimensional facial morphology, Am. J. Hum. Genet. 77 (2005) 999–1010.
[7] P. Hammond, T.J. Hutton, J.E. Allanson, et al., 3D analysis of facial morphology, Am. J. Med. Genet. A 126 (2004) 339–348.
[8] R.C. Hauspie, C. Susanne, E. Defrise-Gussenhoven, Testing for the presence of genetic variance in factors of face measurements of Belgian twins, Ann. Hum. Biol. 12 (1985) 429–440.
[9] L. Kohn, The role of genetics in craniofacial morphology and growth, Annu. Rev. Anthropol. 20 (1991) 261–278.
[10] K. Lee, G. Byatt, G. Rhodes, Caricature effects, distinctiveness, and identification: testing the face-space framework, Psychol. Sci. 11 (2000) 379–385.
[11] D.A. Leopold, I.V. Bondar, M.A. Giese, Norm-based face encoding by single neurons in the monkey inferotemporal cortex, Nature 442 (2006) 572–575.
[12] H.S. Loos, D. Wieczorek, R.P. Wurtz, C. von der Malsburg, B. Horsthemke, Computer-based recognition of dysmorphic faces, Eur. J. Hum. Genet. 11 (2003) 555–560.
[13] K. Ma, T. Xiaoou, Discrete wavelet face graph matching, in: International Conference on Image Processing, Thessaloniki, Greece, vol. 2, 2001, pp. 217–220.
[14] C. Marquet, P.O.S.S.U.M. User's Manual, C.P. Export Pty Ltd., Melbourne, 1987.
[15] J. Peng, H. Deng, C. Cao, M. Ishikawa, Craniofacial morphology in Chinese female twins: a semi-longitudinal cephalometric study, Eur. J. Orthod. 27 (2005) 556–561.
[16] R.M. Winter, What's in a face? Nat. Genet. 12 (1996) 124–129.
[17] R.M. Winter, M. Baraitser, London Dysmorphology Database, Oxford University Press, Oxford, 1990.
[18] L. Wiskott, C. von der Malsburg, Recognizing faces by dynamic link matching, Neuroimage 4 (1996) S14–S18.
[19] I.J. Wundrich, C. von der Malsburg, R.P. Wurtz, Image representation by complex cell responses, Neural Comput. 16 (2004) 2563–2575.